^{13}C, ^{1}H, ^{6}Li Magic-Angle Spinning Nuclear Magnetic Resonance, Electron Paramagnetic Resonance, and Fourier Transform Infrared Study of Intercalation Electrodes Based in Ultrasoft Carbons Obtained below 3100 K

R. Alcántara, F. J. Fernández Madrigal, P. Lavela, and J. L. Tirado*

Laboratorio de Química Inorgánica, Facultad de Ciencias, Universidad de Córdoba, Avda San Alberto Magno, s/n 14004 Córdoba, Spain

J. M. Jiménez Mateos

Repsol Research Center, Embajadores, Madrid, Spain

R. Stoyanova and E. Zhecheva

Institute of General and Inorganic Chemistry, Bulgarian Academy of Sciences, 1113 Sofia, Bulgaria

Received May 19, 1998. Revised Manuscript Received October 6, 1998

Petroleum coke samples of different origins and heat treated at different temperatures below 3100 K have been studied by spectroscopic and electrochemical procedures. According to ^{13}C and ^{1}H magic-angle spinning (MAS) nuclear magnetic resonance (NMR), infrared (IR), and electron paramagnetic resonance (EPR) data, aromatic compounds and surface OH groups are present in green coke samples. The preparation of CMB (combustible) sample from 1673 K leads to a low-temperature graphitization process, as shown by the occurrence of multiphase products containing both turbostratic and graphitized solid. This process is accompanied by the loss of aromatic compounds and surface hydroxyls. The optimization of the lithium intercalation electrodes based in the green coke materials was carried out by thermal treatment at 1023 K under dynamic vacuum conditions. Such pretreatment of the electrode material leads to marked enhancement of reversible capacities without the higher temperatures usually required for other soft carbon materials. Finally, the results of ^{6}Li MAS NMR and EPR have been correlated with the experimental determination of lithium diffusion coefficients and surface properties. On the basis of these results, spin resonance spectroscopies are found to be a powerful tool to discern between the different petroleum coke samples to select the active electrode material with best performance.

Introduction

The past decade has seen an important development of materials for high-performance energy storage systems. Particularly, the field of electrode materials for advanced lithium batteries has attracted the interest of numerous researchers. Since the development of the first commercial lithium ion product,[1,2] an increasing effort was devoted to the improvement of both the positive and the negative electrode materials. To date, the active cathode material with full commercial application is based on the layered oxide $LiCoO_2$.[3,4] Similarly, the commercially most successful anode composition in these cells consists of a carbon active electrode material. Together with clay minerals, graphite intercalation compounds (GIC) are some of the oldest known examples of intercalation chemistry.[5] Graphite can easily intercalate alkali metals because of its layered structure. The adverse effects of the complex staging phenomena and the possible solvent cointercalation processes prevent the use of graphite as lithium intercalation electrode material in nonaqueous electrolyte rechargeable batteries. These undesirable effects are inhibited in other less organized forms of carbon, in which defects play the role of a "pin", thus limiting enhanced interlayer expansion. Consequently, a large number of reports have been published on the electrochemical lithium intercalation properties of hard nongraphitizable carbons and soft carbons heat treated at lower temperatures. Petroleum cokes,[6−9] mesocarbon

* Corresponding author. Telephone: 34957 218637. Fax: 34957 218606. E-mail: iq1ticoj@lucano.uco.es.

(1) Nagaura, T.; Tazawa, K. *Prog. Batt. Sol. Cells.* **1990**, *9*, 20.
(2) Nagaura, T. *Prog. Batts. Batt. Mats.* **1991**, *10*, 209.
(3) Bruce, P. G. *Chem. Commun.* **1997**, 1817.
(4) Zhecheva, E.; Stoyanova, R.; Gorova, M.; Alcántara, R.; Morales, J.; Tirado, J. L. *Chem. Mater.* **1996**, *8*, 1429.
(5) Schlögl, R. In *Progress in Intercalation Research*; Müller-Warmuth, W.; Schöllhorn, R., Eds.; Kluwer: Boston, MA, 1994.
(6) Dahn, J. R.; von Sacken, U.; Juzkow, M. W.; Al-Janaby, H. *J. Electrochem. Soc.* **1991**, *138*, 2207.

10.1021/cm980352t CCC: $18.00
Published on Web 12/11/1998

microbeads,[10] and coal pitch-based carbon powders and fibers[11,12] provide several examples of this application. Among these modifications, petroleum coke offers several advantages related to the low cost of this secondary product of the petrochemical industry. In addition, the interest of the application of cokes in the battery industry is significantly higher from the economic point of view than that derived from the usual applications of this material as a re-carburant or in electrodes for electrolysis of steel or aluminum.

Because of their multiple origins and possible levels of graphitization, the performance of carbon-based intercalation electrodes may vary within a wide range. Detailed studies on the relationships between preparation and thermal treatment and electrode performance have been carried out from which relevant conclusions have been extracted. Parallel efforts have been devoted to the application of spectroscopic techniques such as nuclear magnetic resonance (NMR)[13−19] and electron paramagnetic resonance (EPR)[14,20−21] to correlate more subtle properties of the carbonaceous materials; such as, the electronic state of lithium and carbon during the intercalation process into "special" forms of carbon. Surprisingly, comparatively less attention has been paid to these effects in petroleum coke. Thus, several aspects of the electronic processes associated with the intercalation reaction remain unclear. The aim of this work is to find correlations between the spectroscopic results obtained for different petroleum coke samples heat treated at different temperatures with their electrochemical performance.

Experimental Details

Four green petroleum cokes were supplied by Repsol Petroleum Company, Madrid. These samples were prepared at 753 K in an industrial coker from the following: heavy-oil vacuum residue, sample henceforth referred to as GCMB ("combustible"); light-oil vacuum residue, GREG ("regular"); pyrolysis fuel oil, GRCB ("recarburant"); and fluidized catalytic cracking decanted oil, IM ("intermediate"). The green cokes were heat-treated at different temperatures up to 3073 K under an inert argon atmosphere, leading to samples that will be henceforth referred to as RCBT, IMT, REGT and CMBT, respectively, where T is the preparation temperature in Kelvin.

Room temperature ^{1}H, ^{6}Li, and ^{13}C magic-angle spin (MAS) NMR spectra were recorded on a Bruker ACP-400 spectrometer working at 400.13, 58.89, and 100.61 MHz resonance frequencies, respectively (9.400 T) and at 3.5−5.5 kHz spinning rates. The lithium spectra were referenced to an 1 M LiCl aqueous solution. The carbon spectra were referenced to TKS [sodium 3-(trimethylsilyl)propionate 2,2,3,3-D_4, $(CH_3)_3SiCD_2CD_2$-COONa]. The values of %C NMR were obtained by using the procedure described for the characterization of coke samples by Snape et al.[22] by using the intensity ratio between the signal at ca. 130 ppm ascribable to aromatic carbon and the signal of the TKS standard added in known amounts.

The EPR spectra were registered as the first derivative of the absorption signal with an ERS-220/Q spectrometer (ex-GDR) within the temperature range between 90 and 400 K. The *g*-factors were established with respect to a Mn^{2+}/ZnS standard. The signal intensity was determined by double integration of the experimental EPR spectrum. Recordings at different microwave power were used to distinguish the EPR signals.

Powder X-ray diffraction data (XRD) were obtained with a Siemens D5000 apparatus provided with Cu Kα radiation and graphite monochromator. Transmission electron microscopy (TEM) studies were performed with a JEOL 200CX microscope. Specific surface areas were calculated by the Brunauer−Emmety−Teller (BET) method from N_2 adsorption isotherms at 77 K.

The electrochemical behavior of coke samples was evaluated in lithium cells using carbon cathodes that consisted of 7 mm diameter and ca. 0.25 mm thick pellets containing ca. 10 mg of coke and 5% ethylene−propylene−diene terpolymer binder. Intensiostatic discharge−charge experiments were carried out with a multichannel galvanostat-potentiostat system (McPile) working at a 100 h rate, so that a change (Δx) of 1 in Li_xC_6 would take 100 h (i.e., cell currents of ca. 37 mA). The average lithium content of the cathode material was calculated from the amount of electron charge transferred to the active material, on the assumption that no current flow was due to side reactions.

Results and Discussion

X-ray Diffraction and Specific Surface Area Determinations. The structural changes of coke samples with the temperature of thermal treatment were first evaluated by recording the XRD patterns. To compare the intensities of the reflections in an absolute scale, equal weights of each sample were compacted against a plastic holder with constant volume and exposed surface area. The interval in which the (002) and (004) line profiles of partially crystallized carbonaceous materials are expected is shown in Figure 1 for a selected set of samples. For green cokes, a highly broadened, low-intensity diffraction profile ascribable to a turbostratic material was exclusively observed. For samples prepared between 1673 and 2173 K, two complex diffraction profiles were observed at each region of the diffractogram. They can be ascribed to the overlapping of two profiles with their centroids differing by ca. 0.5° and 1.5° 2θ for (002) and (004) regions, respectively. The simultaneous occurrence of turbostratic and graphitized phases in the structure of cokes prepared at 1673 K was previously reported.[23] The diffraction maximum located at lower spacing can be ascribed to graphitized phases, whereas the profile due

(7) Guyomard, D.; Tarascon, J. M. *J. Electrochem. Soc.* **1992**, *139*, 937.
(8) Dahn, J. R.; Sleigh, A. K.; Shi, H.; Reimers, J. N.; Zhong, Q.; Way, B. M. *Electrochim. Acta* **1993**, *38*, 1179.
(9) Guyomard, D.; Tarascon, J. M. *J. Electrochem. Soc.* **1993**, *140*, 3071.
(10) Inaba, M.; Yoshida, H.; Ogumi *J. Electrochem. Soc.* **1996**, *143*, 2572.
(11) Uchida, T.; Itoh, T.; Morikawa, Y., Ikuta, H., Wakihara, M. *Denki Kagaku* **1993**, *61*, 1390.
(12) Uchida, T.; Morikawa, Y., Ikuta, H., Wakihara, M., Suzuki, K. *J. Electrochem. Soc.* **1996**, *143*, 2606.
(13) Sato, K.; Noguchi, M.; Demachi A.; Oki, N.; Endo, M. *Science* **1994**, *264*, 556.
(14) Tanaka, K.; Ata, M.; Kimura, H.; Imoto, H. *Bull. Chem. Soc. Jpn.* **1994**, *67*, 2430.
(15) Tatsumi, K.; Akai, T.; Imamura, T.; Zaghib, K.; Iwashita, N.; Higuchi, S.; Sawada, Y. *J. Electrochem. Soc.* **1996**, *143*, 1923.
(16) Tatsumi, K.; Conard, J.; Nakahara, M.; Menu, S.; Lauginie, P.; Sawada, Y.; Ogumi, Z. *Chem. Commun.* **1997**, 687.
(17) Hayes, S.; van Wüllen, L.; Eckert, H.; Even, W. R.; Crocker, R. W.; Zhang, Z. *Chem. Mater.* **1997**, *9*, 901.
(18) Takami, N.; Satoh, A.; Ohsaki, T.; Kanda, M. *Electrochim. Acta* **1997**, *42*, 2537.
(19) Nakagawa, Y.; Wang, S.; Matsumura, Y.; Yamaguchi, C. *Synth. Metals* **1997**, *85*, 1363.
(20) Zhuang, L.; Lu, J.; Ai, X.; Yang, H. *J. Electroanal. Chem.* **1995**, *397*, 315.
(21) Matsumura, Y.; Wang, S.; Nakagawa, Y.; Yamaguchi, C. *Synth. Metals* **1997**, *85*, 1411.
(22) Snape, C. E.; McGhee, B. J.; Martin, S. C.; Andresen, J. M. *Catal. Today* **1997**, *37*, 285.
(23) Alcántara, R.; Jiménez-Mateos, J. M.; Lavela, P.; Morales, J.; Tirado, J. L. *Mater. Sci. Eng.* **1996**, *B39*, 216.

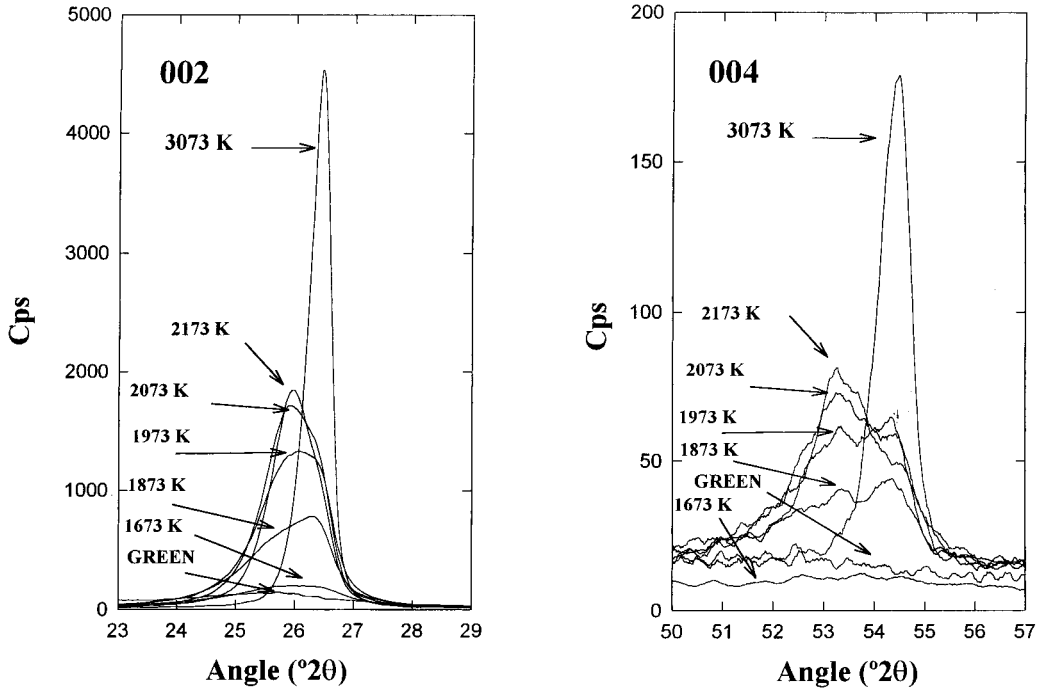

Figure 1. The (002) and (004) XRD line profiles of green petroleum coke GCMB and thermally treated samples.

to the turbostratic phase occurs at higher spacing. On increasing the preparation temperature in the 1673−2173 K range, the diffraction patterns reveal a slight decrease in the relative intensity of the contribution ascribable to graphitized phases. At 3073 K, only a single maximum corresponding to a highly graphitized carbon was observed.

According to previous works,[24] the progressive heating of soft carbonaceous materials between 873 and 1273 K leads to the elimination of hydrogen. Simultaneously, an increase in the size of the graphene sheets takes place. This growth process prevails up to 2273 K without relief of the turbostratic misalignment. This model agrees well with the more crystalline patterns observed for our petroleum coke samples heated at temperatures higher than 1273 K (Figure 1). However, the presence of a two-phase system revealed by XRD and TEM[23] for samples obtained below 2273 K should be interpreted by assuming that the transformation from unorganized carbon to turbostratic material takes place simultaneously with the conversion of the turbostratic solid to graphitized material. Nevertheless, the former process takes place to a larger extent below 2273 K, as shown by the relative intensities of the contributions to the (002) and (004) lines ascribable to both modifications. The fact that graphitization takes place significantly above 1673 K allows us to consider these materials as ultrasoft carbons.

The values of BET surface area at each preparation temperature are collected in Table 1. Particularly low surface areas were detected for both green coke and samples prepared at the higher temperature limit of 3073 K. The different array of carbon atoms in these samples hinders an explanation of the results based on structural similarities. It is evident that graphitization is expected to increase grain size and thus to lower surface areas. However, the low specific surface for the green coke sample can be ascribed to a negligible content of pores, whereas the heating reaction releases gaseous products, as already mentioned, and creates a porous texture that increases the surface of cokes at higher temperatures.

Table 1. Changes in the Specific Surface Area Obtained by the BET Method with Preparation Temperature of Petroleum Coke CMB Samples Thermally Treated at Different Temperatures

T, K	S_{BET}, $m^2\ g^{-1}$
green coke	0.70
1673	5.20
1973	8.70
2073	7.80
2173	4.30
3073	2.68

^{13}C NMR, ^{1}H NMR, and Fourier Transform Infrared (FTIR) of Green Cokes and Heat-Treated Products. It is well-known that ^{13}C NMR studies are always complicated by the low natural abundance of this active isotope (1%) and the low sensitivity of the NMR technique to the resonance of the carbon nucleus, as a result of its low gyromagnetic ratio. When these studies are carried out on graphite and graphite-related materials, the probe detuning effects caused by the moderate-to-high electrical conductivity of these solids give additional difficulties to the recording of an admissible quality spectrum. However, MAS NMR measurements on the precursors of carbonaceous materials provide valuable information. Also, when the amount of impurity atoms is high, cross-polarization (CP) techniques are useful to examine carbon nuclei.[25] The ^{13}C MAS NMR spectra of the green cokes are shown in Figure 2 a−d. The presence of a single resonance signal located at ca. 130 ppm and the corresponding spinning side bands was differentiated by recording the spectra at

(24) Dahn, J. R.; Zheng, T.; Liu, Y.; Xue, J. S. *Science* **1995**, *270*, 590.

(25) Egiebor, N. O.; Gray, M. R.; Cyr, N. *Appl. Catal.* **1989**, *55*, 81.

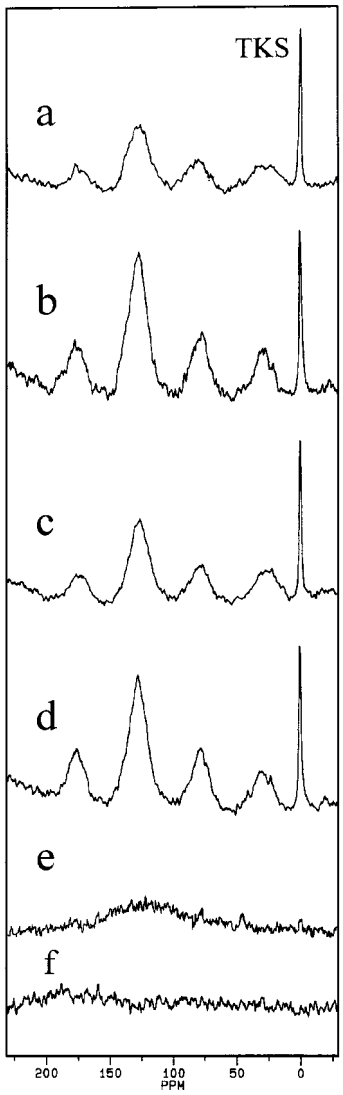

Figure 2. The ^{13}C MAS NMR of (a) GRCB, (b) GCMB, (c) GREG, (d) GIM, (e) RCB1023, and (f) RCB1673.

3500 and 5000 Hz spinning rate. The chemical shift value is indicative of aromatic carbon.[22,25] The CP MAS measurements did not allow to resolve further resonances in the spectra. On the other hand, the ^1H NMR (Figure 3) results reveal a significant proton content in the samples.

The FTIR spectra of the green cokes (Figure 4) agree with the interpretation of the NMR data based on the presence of aromatic groups. A doublet in the 1400−1600 cm^{-1} region and several intense bands in the 700−900 cm^{-1} region are ascribable to aromatic and aliphatic groups. Moreover, FTIR spectra give complementary information to the ^1H NMR data by revealing the presence of OH groups, probably surface groups. These groups have been found in other coke electrodes, and were considered as a negative factor for their reversible capacity.[26]

For coke samples treated at 1673 K, no ^{13}C NMR spectra were observed (Figure 2f), even by using CP and/or MAS techniques. Although the lack of NMR signal could be a consequence of the enhanced conduction

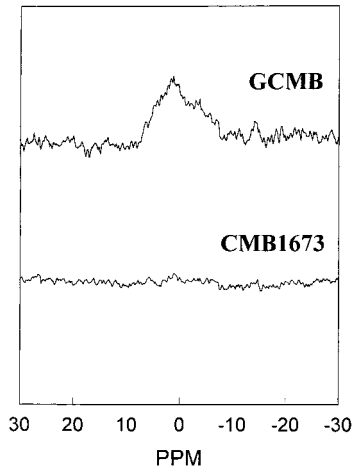

Figure 3. The MAS PMR spectra of GCMB and CMB1673 samples.

properties and the detuning effect of the itinerant electrons, it should be noted that the degree of graphitization is low even in the heat-treated samples and thus, the conduction phenomena should be found within the graphene layers in the turbostratic material. Alternatively, the spectrum in Figure 2e could be indicative that the signals found in the green cokes resulting from non-carbonized materials are converted and/or evolved during the thermal treatment. The ^1H NMR spectra (Figure 3) also agree with this interpretation, as the proton resonance disappears at 1673 K. The evolution in the ^1H NMR spectra evidence the absence of OH groups and organic hydrogen in the heat-treated sample. Similarly, the signals in the FTIR spectra are consistent with this interpretation (Figure 4).

EPR Spectra of Green Cokes and Heat-Treated Products. In attempt to assess the microstructure of green cokes and heat-treated products, EPR spectroscopy was used as an experimental tool. Figures 5 and 6 compare the EPR spectra of green cokes and heat-treated products. The EPR spectra of green petroleum cokes consist of single line with Lorentzian shape and $g = 2.0020 \pm 0.0003$ (Figure 5). The line width slightly increases upon cooling (Table 2). The temperature dependence of the signal intensity obeys the Curie law in the temperature range 100−300 K (Table 2). At one and the same recording temperature, the line width and signal intensity are sensitive toward the type of the samples: the most intense and narrow signals were detected for GRCB and GIM cokes. Moreover, there is an apparent correlation between the line width and signal intensity: the line width increases simultaneously with the decrease in the signal intensity (Table 2).

The EPR data obtained (in terms of *g*-factor, line width, and temperature dependence of the signal intensity) reveal that EPR signal at green petroleum cokes originates from localized paramagnetic centers. At the same time, the EPR signal with the same parameters has been detected at carbonaceous materials heated to 973 K.[27−29] According to Singer et al.,[27,28] this signal

(26) Kikuchi, M.; Ikezawa, Y.; Takamura, T. *J. Electroanal. Chem.* **1995**, *396*, 451.

(27) Singer, L. S. In *Proceeding of the 5th Carbon Conference*; Pergamon: Oxford, 1963; vol. II, p 63.
(28) Singer, L. S.; Lewis, I. C. *Appl. Spectrosc.* **1981**, *36*, 52.
(29) Kawamura, K. *Carbon* **1998**, *36*, 1227.

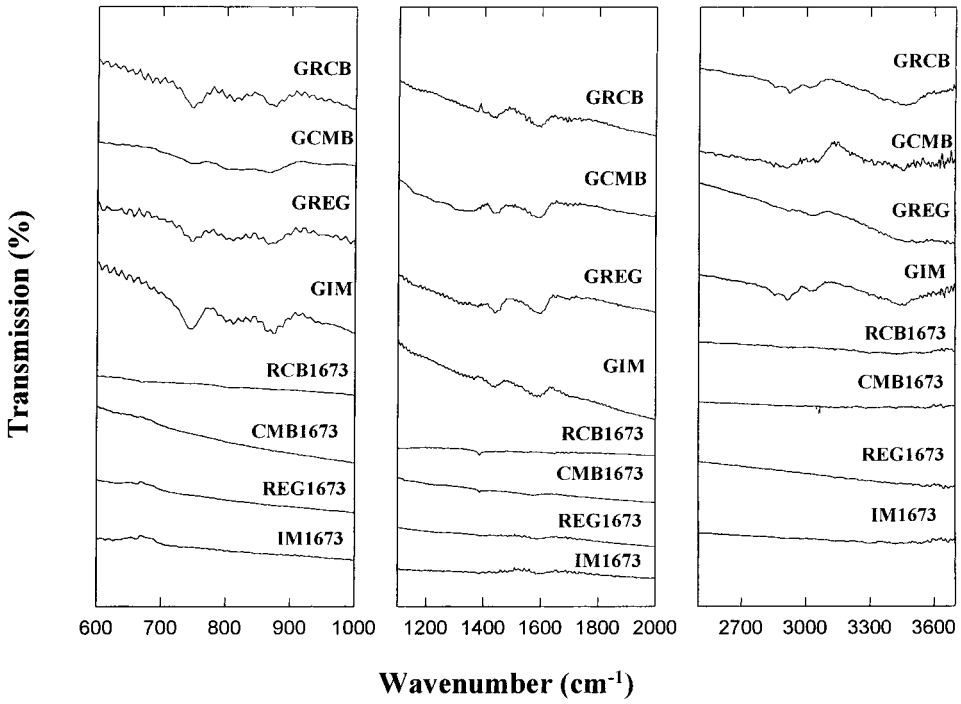

Figure 4. The FTIR spectra of green petroleum coke samples and samples treated at 1673 K.

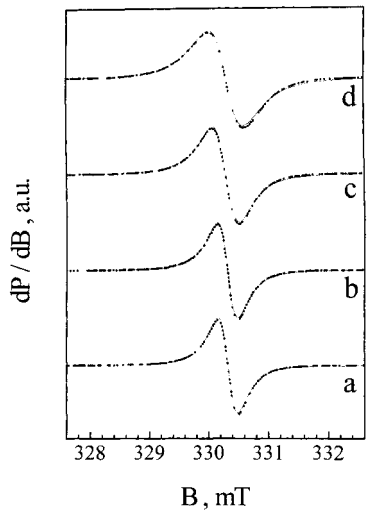

Figure 5. The EPR spectra recorded at 293 K of green petroleum cokes: (a) GIM, (b) GRCB, (c) GREG, and (d) GCMB. The dotted and the full lines correspond to the experimental and simulated spectra, respectively.

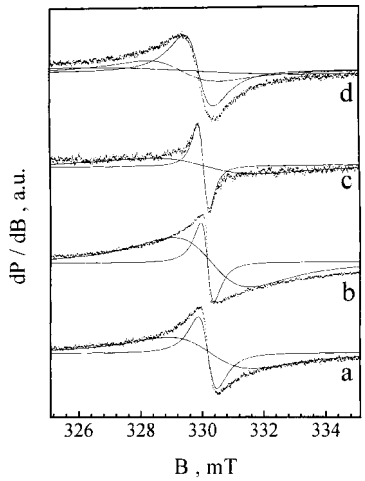

Figure 6. The EPR spectra recorded at 293 K of petroleum cokes treated at 1673 K: (a) IM1673, (b) RCB1673, (c) REG1673, and (d) CMB1673. The dotted and the full lines correspond to the experimental and simulated spectra, respectively.

corresponds to aromatic π-radicals in which the unpaired electron is delocalized over the aromatic rings. This electron motion over aromatic rings accounts for the line shape and line width of the signal. In addition, the exchange interactions between unpaired electrons may also contribute to the EPR line width. Returning to the samples investigated by us, there is an experimental relation between the spin density of the aromatic π-radicals and the total amount of the aromatic carbon determined from ^{13}C MAS NMR data (Table 2). Because the nonprotonated aromatic carbon is usually underestimated in the ^{13}C MAS NMR experiment,[30] it looks like a high-spin density of aromatic π-radicals is observed for green cokes with a high amount of protonated aromatic carbon (Table 2).

For petroleum cokes treated at 1673 K, the EPR spectrum is changed significantly: a narrow Lorentzian, with $g = 2.0028 \pm 0.004$, superimposed on a broad Lorentzian, with $g = 2.0026 \pm 0.0005$, gives rise to the EPR spectra of the samples with the exception of CMB1673 (Figure 6). For CMB1673, three Lorentzians with different line widths determine the EPR profile (Figure 6). The total spin density of the EPR signals for heat-treated products is drastically lower compared with that of the green cokes (Tables 2 and 3). It is interesting to note that the line width of the narrower signal is higher for the CMB coke than that found for the green coke samples. In contrast to the green petroleum cokes, there is no correlation between line width and signal intensity (Table 3). On cooling, the

(30) Snape, C. E.; Axelson, D. E.; Botto, R. E.; Delpuech, J. J.; Tekely, P.; Gerstein, B. C.; Pruski, M.; Maciel, G. E.; Wilson, M. A. *Fuel* **1989**, *68*, 547.

Table 2. EPR Line Width ($\Delta H_{pp} \pm 0.003$ mT), Normalized Intensity (I_T/I_{293}), and Signal Intensity [I (a.u.)] for Green Petroleum Cokes

	GIM			GRCB			GREG			GCMB		
temperature, K	ΔH_{pp}	I_T/I_{293}	I	ΔH_{pp}	I_T/I_{293}	I	ΔH_{pp}	I_T/I_{293}	I	ΔH_{pp}	I_T/I_{293}	I
113	0.361	2.73		0.380	2.52		0.439	2.65		0.590	2.71	
223	0.350	1.25		0.375	1.15		0.439	1.21		0.591	1.22	
293	0.336	1.00	186	0.339	1.00	210	0.420	1.00	156	0.578	1.00	133
%C NMR			13.9			15.1			13.7			10.5

Table 3. EPR Line Widths of Three Lorentzians (ΔH_{pp} − Si1 ± 0.005; ΔH_{pp} − Si2 ± 0.04, and ΔH_{pp} − Si3 ± 0.2 mT), Normalized Intensity (I_T/I_{293}), and Signal Intensity [I(a.u.)] for Petroleum Cokes Treated at 1673 K

	IM1673			RCB1673			REG1673			CMB1673		
parameter	113 K	223 K	293 K	113 K	223 K	293 K	113 K	223 K	293 K	113 K	223 K	293 K
ΔH_{pp} − Sil	0.600	0.593	0.630	0.413	0.417	0.415	0.333	0.349	0.337	0.864	0.863	0.976
I_T/I_{293} − Sil	0.84	1.01	1.00	1.41	∼.17	1.00	1.44	1.14	1.00	0.52	0.91	1.00
I − Sil			0.61			1.00			0.13			0.66
ΔH_{pp} − Si2	2.76	2.71	2.73	2.58	2.80	2.55	3.67	3.57	3.40	1.49	1.86	2.51
I_T/I_{293} − Si2	1.11	1.06	1.00	1.57	1.20	1.00	1.59	1.25	1.00	0.98	1.00	1.00
I − Si2			5.7			20.8			2.8			1.22
ΔH_{pp} − Si3										6.5	7.1	7.0
I_T/I_{293} − Si3										3.15	1.60	1.00
I − Si3												10.9

intensity of the narrower signal for RCB1673 and CMB1673 shows a trend to decrease, whereas for IM1673 and REG1673, the signal intensity increases slightly (Table 3). To the contrary, the intensity of the broader signal increases on cooling, but the Curie−Weiss law is not obeyed (Table 3).

To elucidate the origin of the EPR signals, it should be noted that Zhuang et al.[20] reported a single signal EPR spectra of petroleum coke electrodes, irrespective of particle size. The obtained g-factor of 2.003, near to that of a free electron, suggested conduction electrons. Matsumura et al.[21] found that the EPR spectrum of ribbonlike carbon film consisted of a single line with no hyperfine splitting with a Lorentzian shape and a g-factor of 2.003, suggesting radical spins of π nature. The larger broadening compared with other disordered carbonaceous materials was ascribed to oxygen impurities. Considering the literature EPR data on carbonaceous materials,[20,21,31−34] the results obtained here suggest that delocalized and localized electronic states account for the EPR spectra of petroleum cokes. The narrower signal can be attributed to the conduction electrons, whereas the localized paramagnetic centers contribute mainly to the broad signal. The intermediate signal observed at CMB1673 reflects both the contributions of conduction and localized electrons, the former being higher. Taking into account the coke structure, both EPR signals can be related with graphitized and nongraphitized regions of the heat-treated products. The charge carriers of the graphite-like microcrystallites cause, most probably, the appearance of the narrower Lorentzian (Figure 6). Because the dimensions of these microcrystallites are lower than the microwave skin depth, the EPR line shape is not perturbed by the electrical resistivity of the heat-treated products. It seems that the unpaired localized electrons remain in the nongraphitized regions. Based on the insensitivity of the line width and on the intensity of the broad signal toward the impurity amounts (Table 1, in ref 23). It can be suggested that the paramagnetic centers are localized at defect sites in the carbon skeleton. The observed changes in the concentration and in the line width of localized paramagnetic centers reflect the structural transformation in the unorganized carbon regions during the thermal treatment.

Optimization of the Electrochemical Properties of Green Cokes. From the results just presented, it is expected that the electrochemical behavior of green petroleum cokes should be poor, especially as a result of the presence of organic material isolating the graphene layers from the electrolyte and adsorbed hydroxyl ions that could give irreversible reactions. In fact, the first galvanostatic cycle of green coke electrodes showed an enhanced polarization (Figure 7). On the other hand, it is well established that thermal treatment of soft carbons above 2273 K dramatically improves their performance as lithium intercalation electrodes. Nevertheless, these thermal treatments are an expensive procedure. Due to the ultrasoft nature of the materials studied here, attempts were carried out to improve the performance by using an alternative treatment at lower temperatures under dynamic vacuum. Two different temperatures were chosen: 473 K for samples previously obtained at 1673 K and 1023 K for green cokes. The reversible capacity increased dramatically, especially for green cokes treated at 1023 K (Figure 7). In the case of the samples obtained at 1673 K, the difference affects the irreversible capacity almost exclusively. This parameter decreases significantly after treatment at 473 K under vacuum, probably as a consequence of the irreversible consumption of lithium in the reaction with hydroxyl groups. Spectroscopic measurements shed new light on the changes induced by the thermal treatment under vacuum.

After vacuum treatment of green cokes at 1023 K, the intensity of the EPR signal corresponding to the aromatic π-radicals drastically decreases: from $I = 133$ to $I \sim 0.3$ for GCMB (Figure 8A). For GCMB, the extremely low intensity of the Lorentzian enables detection of the metal impurity ions in cokes (Figure 8B). For GRCB, an axially symmetric signal is visible instead of

(31) Mulay, L. N.; Prasad Rao, A. V.; Rivera-Utrilla, J.; Walker, P. L.; Vannice, M. A. *Carbon* **1985**, *23*, 493.
(32) Boyer, S. J.; Clarkson, R. B. *Colloids Surf.* **1994**, *A82*, 217.
(33) Byszewski, P.; Nabialek, A. *Europhys. Lett.* **1996**, *34*, 31.
(34) Adriaanse, L. J.; Brom, H. B.; Michels, M. A. J.; Brokken-Zijp, J. C. M. *Phys. Rev. B* **1997**, *55*, 9383.

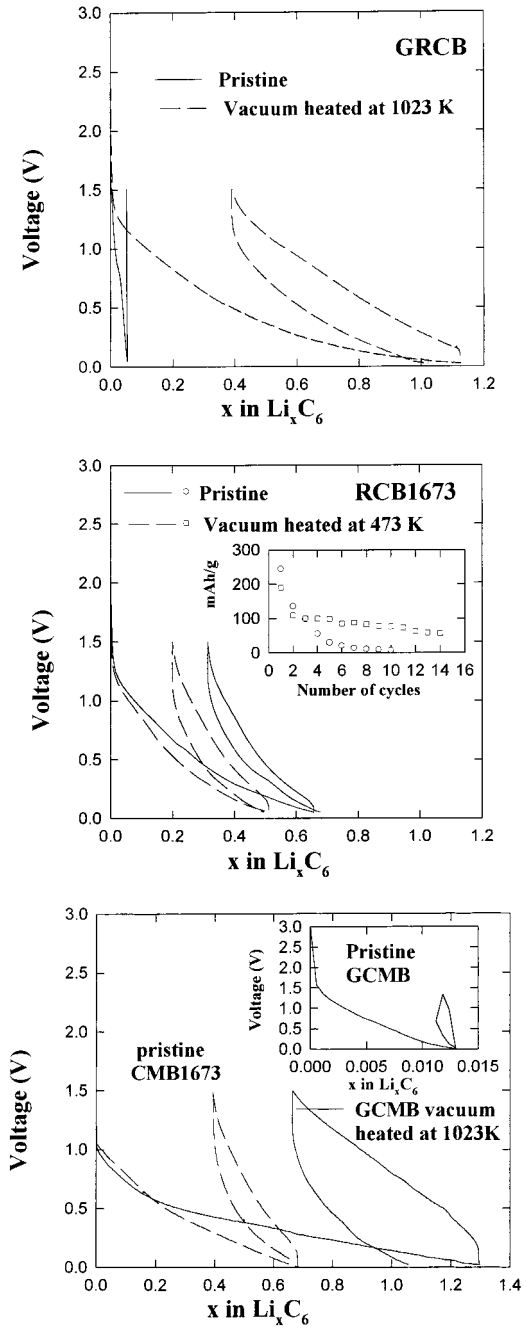

Figure 7. Charge−discharge cycles of GRCB, GCMB, RCB1673, and CMB1673 before an after thermal treatment in a vacuum.

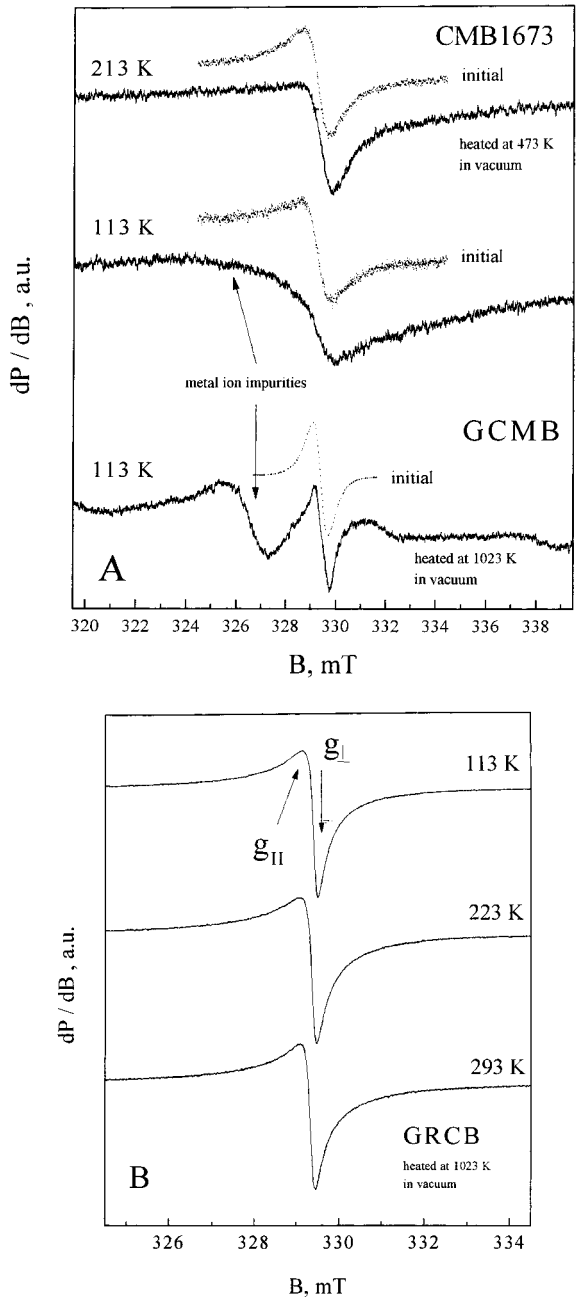

Figure 8. (A) The EPR spectra of vacuum-treated GCMB and CMB1673 cokes. Dotted lines correspond to the untreated pristine cokes. (B) The EPR spectra of vacuum-treated GRCB.

the Lorentzian line: $g_\perp \sim 2.004$ and $g_{||} \sim 2.006$ (Figure 8B). Nevertheless, the Curie law satisfactorily fits the temperature dependence of the intensity of this signal: $I_{113}/I_{293} = 2.67$, $I_{213}/I_{293} = 1.46$, and $I_{293}/I_{293} = 1$. At the same time, the intensity of the axially symmetric signal is about three times lower compared with the Lorentzian of the initial sample: from $I = 210$ to $I = 61$. Having in mind the g-values and the temperature dependence of the intensity of the axially symmetric signal, it seems that the additional signal in vacuum-treated green coke samples originates also from organic radicals. Obviously, these radicals are not stable when the GRCB cokes are exposed in air.

After vacuum treatment at 473 K of CMB1673 cokes, the total intensity of the three Lorentzians decreases ($I_1 + I_2 + I_3 = 12.8$ for initial CMB versus $I_t = 0.2$ for vacuum-treated CMB), but the EPR line envelope remain nearly the same (Figure 8A). As for the vacuum-treated GCMB, the metal ion impurities also contribute to the EPR spectrum of vacuum-treated CMB1673.

For vacuum-treated RCB1673, the EPR spectrum is also changed: it looks like an axially symmetric signal is superimposed on the spectrum of the untreated samples (Figure 9 a and b). As one can see, the axially symmetric signals observed in a vacuum-treated RCB1673 and GRCB are quite similar (in terms of g-values). It is interesting to note that the axially symmetric signal corresponding to organic radicals appears in cokes with different degree of carbonization (GRCB and RCB1673). Summarizing, it seems that vacuum treatment allows a better differentiating of the different kinds of petroleum cokes by EPR.

^{6}Li MAS NMR and EPR of the Discharged Electrodes. Different authors have studied the ^{7}Li MAS

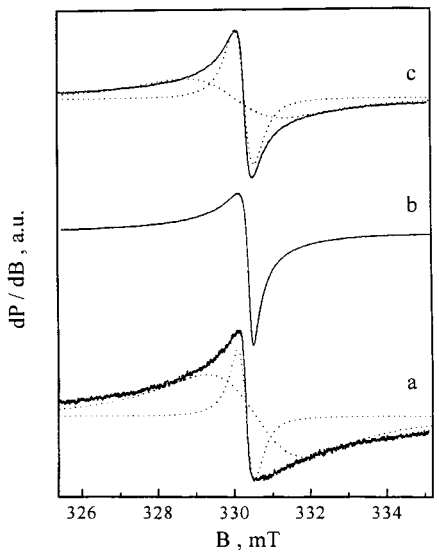

Figure 9. The EPR spectra of RCB1673 cokes: (a) pristine; (b) vacuum treated; and (c) after lithium discharge to 0 V versus Li. Dotted lines correspond to the simulated spectra.

NMR spectra of discharged carbon electrodes: Sato et al.[13] observed a main band around 0 ppm, as referred to LiCl, with fine structure in Li-doped poly(*p*-phenylene)-based disordered carbon. The superposition of three bands to the shape of the main band was ascribed to the presence of doping ionic sites, covalent Li_2 molecules, and byproduct lithium carbonate. Tanaka et al.[14] studied the ^{7}Li NMR spectra in a nongraphitizable ex-poly(furfuryl alcohol) carbon electrode. The existence of the doped lithium in a nonmetallic state with low electron density up to the fully doped case was shown. For lithiated mesocarbon microbeads, Tatsumi et al.[15] observed two signals in the ^{7}Li NMR spectra of the material treated at 2273 K. These bands were centered at 45 and 27 ppm and were ascribed to a first-stage lithium graphite intercalation compound and to the fully lithiated phase of the turbostratic structure. The lithiated product derived from the carbon materials heated at 1023 K showed a band at 7 ppm characteristic of an ionic character. The idea of formation of lithium ion clusters was dismissed in these materials. Instead, the formation of an ionic complex such as lithium naphthalene was suggested. More recently, Tatsumi et al.[16] reported the ^{7}Li NMR spectra of a lithiated nongraphitizable carbon fiber measured below 200 K. Three signals were observed in these materials. An intense band at 18 ppm was ascribed to the lithium species in crystalline graphene layers in the carbon fiber. The other two signals showed a temperature dependence of the NMR shifts. The high shifts of these signals suggested a metallic character of lithium clusters located in the microcavities of the nongraphitizable carbon fiber.

Hayes et al.[17] studied the ^{7}Li MAS NMR spectra of the amorphous carbon-based anode materials generated from pyrolysis of poly(methacrylonitrile/divinylbenzene) copolymers. Three signal components were found in the spectra. A signal at ca. −1 ppm was attributed to isotropically mobile lithium species. A broader signal in the same chemical shift region was ascribed to byproduct lithium carbonate or hydroxide. The band located at the highest shifts was considered not to be attributable to Li_2 dimer species. Takami et al.[18] found

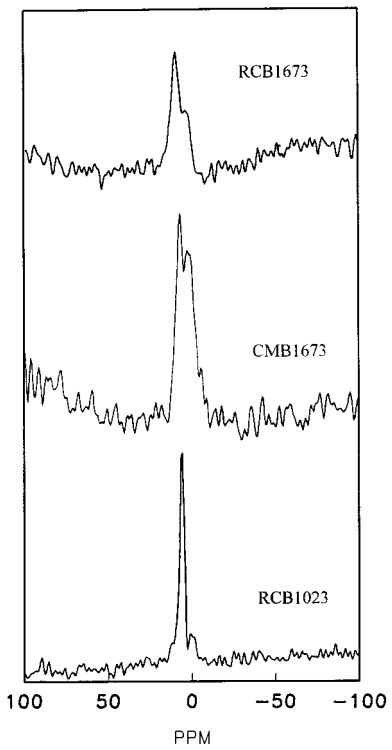

Figure 10. The ^{6}Li MAS NMR of RCB1023, RCB1673, and CMB1673 electrodes after lithium intercalation to 0 V.

Table 4. Chemical Shifts (δ) and Intensity Ratios of Different Coke Samples and Thermal Treatments

sample	δ_1	δ_2	$I(\delta_1)/I(\delta_2)$
RCB1673	0.91	9.51	1.82
CMB1673	0.45	8.52	1.27
RCB1023	0.47	7.82	4.67

two signals with low shifts in the ^{7}Li NMR spectra of perylene-based disordered carbons after lithiation that were ascribed to the coexistence of the ionic lithium stored in the reversible storage sites and lithium trapped in the irreversible storage sites. Recently, Nakagawa et al.[19] observed that the Knight shift of one of the two signals in the ^{7}Li NMR spectra of an isotropic pitch carbon-based electrode, which was ascribable to inserted lithium, increases with Li concentration. The authors suggest that with increasing the lithium species concentration during the intercalation process, the electron spin density at the Li nucleus increases.

On the other hand, it is known that ^{6}Li NMR offers a higher resolution than ^{7}Li NMR in lithium insertion compounds, although penalized by a lower sensitivity.[35−37] The experimental ^{6}Li MAS NMR spectra of three selected samples are shown in Figure 10. A relationship between the relative intensity of the two signals with the ratio between reversible and irreversible capacity (Figure 7) of these electrode materials was observed (Table 4). Thus, the higher intensity of the signal closer to 0 ppm is ascribable to a larger content of ionic forms of lithium with isotropic mobility, such

(35) Hirschinger, J.; Mongrelet, T.; Marichal, C.; Granger, P.; Savariault, J. M.; Déramond, E.; Galy, J. *J. Phys. Chem.* **1993**, *97*, 10301.
(36) Marichal, C.; Hirshinger, J.; Granger, P.; Ménétrier, M.; Rougier, A.; Delmas, C. *Inorg. Chem.* **1995**, *34*, 1773.
(37) Stoyanova, R.; Zhecheva, E.; Alcántara, R.; Lavela, P.; Tirado, J. L. *Solid State Commun.* **1997**, *102*, 457.

as lithium carbonate, which are expected to be formed during the generation of the SEI layer. On the contrary, the signal shifted to higher ppm reveals inserted lithium in which the electron spin density at the lithium nucleus is increased. It should be noted that the higher intensity of the positive shift signal is observed for the sample heat treated in a vacuum at 1023 K (Figure 10 and Table 4), which in turn showed an enhanced electrode capacity compared with the original green petroleum coke (Figure 7).

Further insight into the electron structure of the lithium-inserted carbons can be obtained by EPR analysis of petroleum cokes used as electrode materials in lithium cells. Figure 9c shows the EPR spectrum of RCB1673 in discharged state to 0 V versus lithium metal, after four cycles of discharge−charge where the electrode has a stoichiometry of $Li_{0.4}C_6$. After lithium insertion in RCB1673, the axially symmetrical signal disappears. The EPR spectra of $Li_{0.4}C_6$ is a superposition of two Lorentzians, as in the case of untreated pristine RCB1673 (Figure 9a, Table 5). In comparison with the EPR parameters of untreated pristine RCB1673, the line widths of both signal decrease slightly, whereas there is an increase and a decrease in the intensities of the narrower and broader Lorentzians, respectively (Table 3). The observed changes in the intensities of the EPR signals mean that lithium insertion in petroleum cokes increases the number of conduction electrons, whereas the paramagnetic defects (aromatic radicals and defect sites in the carbon framework) play a role as electron acceptors.

Table 5. EPR Line Widths of Two Lorentzians (ΔH_{pp} − Si1 ± 0.005 and ΔH_{pp} − Si2 ± 0.04 mT), Normalized Intensity (I_T/I_{293}), and Signal Intensity [*I*(a.u.)] for Pristine RCB1673 and RCB1673 after Four-Cycles of Charge−Discharge with a $Li_{0.4}C_6$ Stoichiometry

	RCB, pristine			RCB, electrode		
parameter	113 K	223 K	293 K	113 K	223 K	293 K
ΔH_{pp} − Si1	0.413	0.417	0.415	0.382	0.372	0.352
I_T/I_{293} − Si1	1.41	1.17	1.00	0.96	0.99	1.00
I − Si1			1.00			1.78
ΔH_{pp} − Si2	2.58	2.80	2.55	1.75	1.77	1.77
I_T/I_{293} − Si2	1.57	1.20	1.00	1.74	1.25	1.00
I − Si2			20.8			10.3

Acknowledgment. The authors acknowledge financial support of CE (contract JOU2-CT93-0326 and supplementary agreement CIPD-CT94-0501). The authors also express their gratitude toward CICYT (contract PB95-0561) for meeting publication costs, Instituto Andaluz de Química Fina for X-ray diffraction facilities, and Servicio de RMN (University Córdoba). E.Zh. and R.St. are indebted for partial financial support from National Research Foundation of Bulgaria.

CM980352T